PERGAMON

International Journal of Heat and Mass Transfer 45 (2002) 4949–4955

International Journal of HEAT and MASS TRANSFER

www.elsevier.com/locate/ijhmt

Effect of local thermal non-equilibrium on thermally developing forced convection in a porous medium

D.A. Nield [a,*], A.V. Kuznetsov [b], Ming Xiong [b]

[a] Department of Engineering Science, University of Auckland, Private Bag 92019, Auckland, New Zealand

[b] Department of Mechanical and Aerospace Engineering, North Carolina State University, Campus Box 7910, Raleigh, NC 27695-7910, USA

Received 14 March 2002; received in revised form 24 May 2002

Abstract

The classical Graetz methodology is applied to investigate the effect of local thermal non-equilibrium on the thermal development of forced convection in a parallel-plate channel filled by a saturated porous medium, with walls held at constant temperature. The Brinkman model is employed. The analysis leads to an expression for the local Nusselt number, as a function of the dimensionless longitudinal coordinate, the Péclet number, the Darcy number, the solid–fluid heat exchange parameter, the solid/fluid thermal conductivity ratio, and the porosity.

1. Introduction

The problem of forced convection in a porous medium channel or duct is a classical one (at least for the case of slug flow (Darcy model)). There has recently been renewed interest in the problem of forced convection in a porous medium channel because of the use of hyperporous media in the cooling of electronic equipment. Recent surveys have been made by Nield and Bejan [1] and by Lauriat and Ghafir [2]. Until recently the discussion of thermally developing convection has been confined to the case of slug flow, which is appropriate on the Darcy model. For the case of highly porous media, the Brinkman model is appropriate. Using this model Nield et al. [3,4] have analyzed the thermal development for the cases of a parallel-plate channel or a circular tube, with the walls being held either at uniform temperature or at constant heat flux. These analyses have been made on the assumption of local thermal equilibrium between the fluid and solid materials in the porous medium.

This paper is concerned with the more general situation when there is no longer local thermal equilibrium. Industrial examples are the cooling of rods in nuclear reactors and solar energy storage systems; for references see [5]. For this case, the fully developed situation has been treated by Nield [5] and Nield and Kuznetsov [6], but for the Darcy case only. The present work is essentially a composite of the work discussed in [3,5]. For simplicity, we concentrate on the case of a parallel-plate channel with uniform temperature on the boundary walls. For completeness, we record that a related numerical study has been reported by Amiri and Vafai [7].

2. Analysis

2.1. Basic equations

We use asterisks to denote dimensional variables. For the steady-state hydrodynamically developed situation we have unidirectional flow in the x^*-direction between impermeable boundaries at $y^* = -H$ and $y^* = H$, as illustrated in Fig. 1. The temperature on each boundary is held constant at the value T_w. At $x = 0$ the inlet temperature T_{IN} is assumed constant.

* Corresponding author. Tel.: +64-9-3737-599; fax: +64-9-3737-468.

E-mail address: d.nield@auckland.ac.nz (D.A. Nield).

0017-9310/02/$ - see front matter
PII: S0017-9310(02)00203-X

Nomenclature

c_P	specific heat at constant pressure ($\mathrm{J\,kg^{-1}\,K^{-1}}$)
C_n, D_n	coefficients defined by Eqs. (33)–(36)
Da	Darcy number, K/H^2
$F_n(y)$, $S_n(y)$	eigenfunctions
G	applied pressure gradient ($\mathrm{N\,m^{-3}}$)
h	heat transfer coefficient ($\mathrm{W\,m^{-2}\,K^{-1}}$)
h_{fs}	specific fluid–solid heat transfer coefficient ($\mathrm{W\,m^{-3}\,K^{-1}}$)
H	half channel width (m)
k	fluid thermal conductivity ($\mathrm{W\,m^{-1}\,K^{-1}}$)
k_r	thermal conductivity ratio, k_s/k_f
K	permeability ($\mathrm{m^2}$)
M	μ_{eff}/μ
Nu	local Nusselt number defined by Eq. (38)
$\overline{Nu}$	mean Nusselt number defined by Eq. (41b)
N_h, N_f, N_s	parameters defined in Eq. (19)
Pe	Péclet number defined by Eq. (17)
q''	wall heat flux ($\mathrm{W\,m^{-2}}$)
S	$(M\,Da)^{-1/2}$
T^*	temperature (K)
T_{IN}	inlet temperature (K)
$T_{b,eff}$	effective bulk mean temperature (K)
T_w	wall temperature (K)
u	$\mu u^*/GH^2$
u^*	filtration velocity ($\mathrm{m\,s^{-1}}$)
$\hat{u}$	u^*/U
U	mean velocity defined by Eq. (6) ($\mathrm{m\,s^{-1}}$)
x	x^*/PeH
x^*	longitudinal coordinate (m)
y	y^*/H
y^*	transverse coordinate (m)

Greek symbols

η	fluid–solid heat exchange parameter
θ	$(T^* - T_w)/(T_{IN} - T_w)$
λ_n	eigenvalues
μ	fluid viscosity ($\mathrm{kg\,m^{-1}\,s^{-1}}$)
μ_{eff}	effective viscosity in the Brinkman term ($\mathrm{kg\,m^{-1}\,s^{-1}}$)
ρ	fluid density ($\mathrm{kg\,m^{-3}}$)
ϕ	porosity

Subscripts

b	bulk
eff	effective
f	fluid
ref	reference
s	solid
w	wall

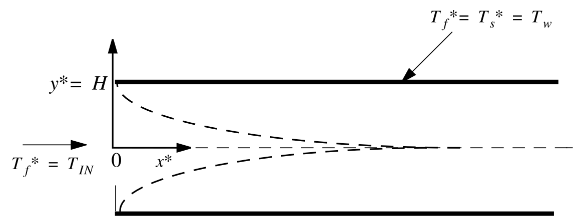

Fig. 1. Definition sketch.

The Brinkman momentum equation is

$$\mu_{eff}\frac{d^2u^*}{dy^{*2}} - \frac{\mu}{K}u^* + G = 0, \tag{1}$$

where μ_{eff} is an effective viscosity, μ is the fluid viscosity, K is the permeability, and G is the applied pressure gradient.

We define dimensionless variables

$$y = \frac{y^*}{H}, \quad u = \frac{\mu u^*}{GH^2}. \tag{2}$$

The dimensionless form of Eq. (2) is

$$M\frac{d^2u}{dy^2} - \frac{u}{Da} + 1 = 0. \tag{3}$$

The solution of this equation subject to the boundary condition $u = 0$ at $y = 1$, and the symmetry condition $du/dy = 0$ at $y = 0$ is

$$u = Da\left(1 - \frac{\cosh Sy}{\cosh S}\right), \tag{4}$$

where

$$S = \left(\frac{1}{MDa}\right)^{1/2}. \tag{5}$$

The mean velocity U is defined by

$$U = \frac{1}{H}\int_0^H u^*\,dy^*. \tag{6}$$

A further dimensionless variable is defined by

$$\hat{u} = \frac{u^*}{U}. \tag{7}$$

This implies that

$$\hat{u} = \frac{S}{S - \tanh S}\left(1 - \frac{\cosh Sy}{\cosh S}\right). \tag{8}$$

We assume that the Péclet number is sufficiently large for axial conduction to be neglected. We also assume that T_s^* and T_f^* are governed by the steady-state heat transfer (energy) equations ([1], Eqs. (6.54), (6.55))

$$(1-\phi)\nabla(k_s\nabla T_s^*) + h_{fs}(T_f^* - T_s^*) = 0, \tag{9}$$

$$\phi\nabla(k_f\nabla T_f^*) + h_{fs}(T_s^* - T_f^*) = (\rho c_P)_f \mathbf{v}^*\nabla T_f^*. \tag{10}$$

Here h_{fs} is a specific fluid–solid heat transfer coefficient, related to a standard heat transfer coefficient h by $h_{fs} = a_{fs}h$, where a_{fs} is the specific surface area. (See Section 2.2.2 of [1].) We define

$$\theta_f^* = T_f^* - T_w, \quad \theta_s^* = T_s^* - T_w. \tag{11}$$

For the case of unidirectional flow in the axial direction, where the Darcy velocity $\mathbf{v}^*$ has the value u^* in the axial direction, and when axial conduction is neglected, Eqs. (9) and (10) reduce to

$$\left[(1-\phi)k_s\frac{\partial^2}{\partial y^{*2}} - h_{fs}\right]\theta_s^* + h_{fs}\theta_f^* = 0, \tag{12}$$

$$\left[\phi k_f\frac{\partial^2}{\partial y^{*2}} - h_{fs} - (\rho c_P)_f u^*\frac{\partial}{\partial x^*}\right]\theta_f^* + h_{fs}\theta_s^* = 0. \tag{13}$$

Eqs. (12) and (13) must be solved subject to the wall boundary conditions

$$\theta_f^* = \theta_s^* = 0 \quad \text{at } y^* = H, \tag{14}$$

the symmetry conditions

$$\frac{\partial\theta_f^*}{\partial y^*} = \frac{\partial\theta_s^*}{\partial y^*} = 0 \quad \text{at } y^* = 0, \tag{15}$$

and the inlet condition

$$\theta_f^* = \theta_{IN} \quad \text{at } x^* = 0. \tag{16}$$

Dimensionless variables are now introduced, with H taken as length scale and θ_{IN} as the temperature scale. We will present our results in terms of a Nusselt number (defined in Eq. (38) below), the porosity ϕ, and four other dimensionless parameters, namely a Péclet number, Pe, a porous medium conductivity ratio, k_r, and a solid–fluid heat exchange parameter, η, defined as follows:

$$Pe = UH(\rho c_P)_f/k_f, \quad k_r = k_s/k_f, \quad \eta = h_{fs}H^2/k_{eff}, \tag{17}$$

where

$$k_{eff} = \phi k_f + (1-\phi)k_s. \tag{18}$$

(The parameter η is related to the Sparrow number Sp introduced by Minkowycz et al. [8] by $\eta = Sp/4$.)

For convenience, we perform the algebra in terms of the parameters

$$N_f = \phi/Pe, \quad N_s = (1-\phi)k_r/Pe,$$
$$N_h = \eta[\phi + (1-\phi)k_r]/Pe. \tag{19}$$

Dimensionless variables are defined by

$$x = x^*/PeH, \quad y = y^*/H, \quad \theta_f = \theta_f^*/\theta_{IN}, \quad \theta_s = \theta_s^*/\theta_{IN}. \tag{20}$$

Then one gets

$$[N_s\partial^2/\partial y^2 - N_h]\theta_s + N_h\theta_f = 0, \tag{21}$$

$$N_h\theta_s + [N_f\partial^2/\partial y^2 - N_h - \hat{u}\partial/\partial x]\theta_f = 0, \tag{22}$$

$$\theta_f = 0 \quad \text{and} \quad \theta_s = 0 \text{ at } y = 1, \tag{23}$$

$$\partial\theta_f/\partial y = 0, \quad \partial\theta_s/\partial y = 0 \quad \text{at } y = 0, \tag{24}$$

$$\theta_f = 1 \quad \text{at } x = 0. \tag{25}$$

Since the differential equations (21) and (22) and the boundary conditions (23) and (24) are all homogeneous, we can immediately separate the variables. We write

$$\theta_f = F(y)e^{-\lambda^2 x}, \quad \theta_s = S(y)e^{-\lambda^2 x}. \tag{26}$$

Then we have an eigenvalue problem constituted by

$$N_sS'' - N_hS + N_hF = 0, \tag{27}$$

$$N_fF'' - N_hF + \lambda^2\hat{u}F + N_hS = 0, \tag{28}$$

$$F'(0) = 0, \quad S'(0) = 0, \quad F(1) = 0, \quad S(1) = 0. \tag{29}$$

Here the primes denote derivatives with respect to y.

Eigenvalues are denoted by λ_n and the corresponding eigenfunction pairs by $F_n(y)$, $S_n(y)$ for $n = 1, 2, 3, \ldots$ In particular,

$$N_sS_n'' - N_hS_n + N_hF_n = 0, \tag{30}$$

$$N_fF_n'' - N_hF_n + \lambda_n^2\hat{u}F_n + N_hS_n = 0. \tag{31}$$

For the LTNE case one no longer has a Sturm–Liouville system to deal with, but from Eqs. (30) and (31), and the corresponding boundary conditions, it is still easy to establish the orthogonality result

$$\int_0^1 \hat{u}F_mF_n\,dy = 0 \quad \text{if } m \neq n. \tag{32}$$

It is noteworthy that the S_n are not involved in this condition.

The general solution of Eqs. (27)–(29) is the pair of series

$$\theta_f = \sum_{n=1}^{\infty} C_nF_n(y)\exp(-\lambda_n^2 x), \tag{33}$$

$$\theta_s = \sum_{n=1}^{\infty} D_nS_n(y)\exp(-\lambda_n^2 x), \tag{34}$$

where the constants C_n are determined by the entrance condition (25). Using the orthogonality condition (32) it follows that

$$C_n = \frac{\int_0^1 \hat{u} F_n \,\mathrm{d}y}{\int_0^1 \hat{u} F_n^2 \,\mathrm{d}y}. \tag{35}$$

With the solution for θ_f completed, one can obtain θ_s from Eq. (22). One quickly finds that

$$D_n = C_n. \tag{36}$$

With the temperature distribution completely found, one can then compute the heat transfer. Matching the heat flux at the channel wall gives

$$q'' = \phi k_\mathrm{f}(\partial T_\mathrm{f}^*/\partial y^*)_{y^*=H} + (1-\phi)k_\mathrm{s}(\partial T_\mathrm{s}^*/\partial y^*)_{y^*=H}. \tag{37}$$

Following Nield and Kuznetsov [6] the Nusselt number is defined by

$$Nu = 2Hh/k_\mathrm{eff}, \tag{38}$$

where, in turn,

$$h = q''/(T_\mathrm{w} - T_\mathrm{b,eff}), \tag{39}$$

where the effective bulk temperature

$$\begin{aligned} T_\mathrm{b,eff} &= \frac{1}{UH}\int_0^H u^*\{\phi T_\mathrm{f}^* + (1-\phi)T_\mathrm{s}^*\}\,\mathrm{d}y^* \\ &= \frac{1}{H}\int_0^H \hat{u}\{\phi T_\mathrm{f}^* + (1-\phi)T_\mathrm{s}^*\}\,\mathrm{d}y^*. \end{aligned} \tag{40}$$

It follows that

$$\begin{aligned} Nu &= \frac{2\{\phi k_\mathrm{f}(\partial\theta_\mathrm{f}/\partial y)_{y=1} + (1-\phi)k_\mathrm{s}(\partial\theta_\mathrm{s}/\partial y)_{y=1}\}}{k_\mathrm{eff}\int_0^1 \hat{u}[\phi\theta_\mathrm{f} + (1-\phi)\theta_\mathrm{s}]\,\mathrm{d}y} \\ &= \frac{2\sum_{n=1}^\infty C_n\{\phi k_\mathrm{f} F_n'(1) + (1-\phi)k_\mathrm{s} S_n'(1)\}\mathrm{e}^{-\lambda_n^2 x}}{k_\mathrm{eff}\sum_{n=1}^\infty C_n\left[\int_0^1 \hat{u}\{\phi F_n + (1-\phi)S_n\}\,\mathrm{d}y\right]\mathrm{e}^{-\lambda_n^2 x}}, \end{aligned} \tag{41}$$

where, from Eqs. (30) and (31),

$$\begin{aligned} F_n'(1) &= \frac{1}{N_\mathrm{f}}\left\{N_\mathrm{h}\int_0^1 (F_n - S_n)\,\mathrm{d}y + \int_0^1 \lambda_n^2 \hat{u} F_n\,\mathrm{d}y\right\}, \\ S_n'(1) &= \frac{-N_\mathrm{h}}{N_\mathrm{s}}\int_0^1 (F_n - S_n)\,\mathrm{d}y. \end{aligned} \tag{42a, b}$$

In order to express our results in terms of k_r we can also use

$$k_\mathrm{f}/k_\mathrm{eff} = 1/\{\phi + (1-\phi)k_\mathrm{r}\}, \tag{43a}$$

$$k_\mathrm{s}/k_\mathrm{eff} = k_\mathrm{r}/\{\phi + (1-\phi)k_\mathrm{r}\}. \tag{43b}$$

This gives the local Nusselt number. The mean Nusselt number, averaged over a length x, is

$$\overline{Nu} = \frac{1}{x}\int_0^x Nu\,\mathrm{d}x. \tag{44}$$

3. Calculations

In order to calculate the eigenvalues and eigenfunctions, it is convenient to express the system (27)–(29) as a system of four first-order equations by writing $y_1 = F$, $y_2 = F'$, $y_3 = S$, $y_4 = S'$, where a prime now denotes a derivative with respect to x. Then

$$\begin{aligned} y_1' &= y_2, \\ y_2' &= -\frac{\lambda^2\hat{u}}{N_\mathrm{f}}y_1 + \frac{N_\mathrm{h}}{N_\mathrm{f}}(y_1 - y_3), \\ y_3' &= y_4, \\ y_4' &= \frac{N_\mathrm{h}}{N_\mathrm{s}}(-y_1 + y_3). \end{aligned} \tag{45a–d}$$

These equations may be solved by a shooting procedure. Each eigenfunction may be normalized by the requirement that it satisfies the condition $F(0) = 1$. Then we have

$$\begin{aligned} &y_1(0) = 1, \quad y_2(0) = 0, \\ &y_3(0) = \mu, \quad y_4(0) = 0. \end{aligned} \tag{46a–d}$$

Starting with an estimate for the values of λ and μ, one can step forward from $x = 0$ to $x = 1$ and vary the values of λ and μ to satisfy the conditions $y_1(1) = 0$, $y_3(1) = 0$, simultaneously. This yields the precise eigenvalue, and the corresponding functions $y_1(x)$ and $y_3(x)$ constitute the required eigenfunction. Once the eigenvalues and eigenfunctions have been obtained, the various other quantities can be obtained by simple numerical integration of the integrals that are involved, and the solution is readily completed. The problem becomes singular as the horizontal coordinate tends to zero, and so for small values of this coordinate each infinite series converges slowly. Then one must take a large number of terms in the series (we were able to handle several hundreds of them) and suffer some loss of accuracy, but this was only a minor inconvenience.

4. Results and discussion

There is potentially a vast parameter range to explore, but we found that the calculations for small values of Pe and large values of η are particularly difficult because of failure of numerical convergence. Conse-

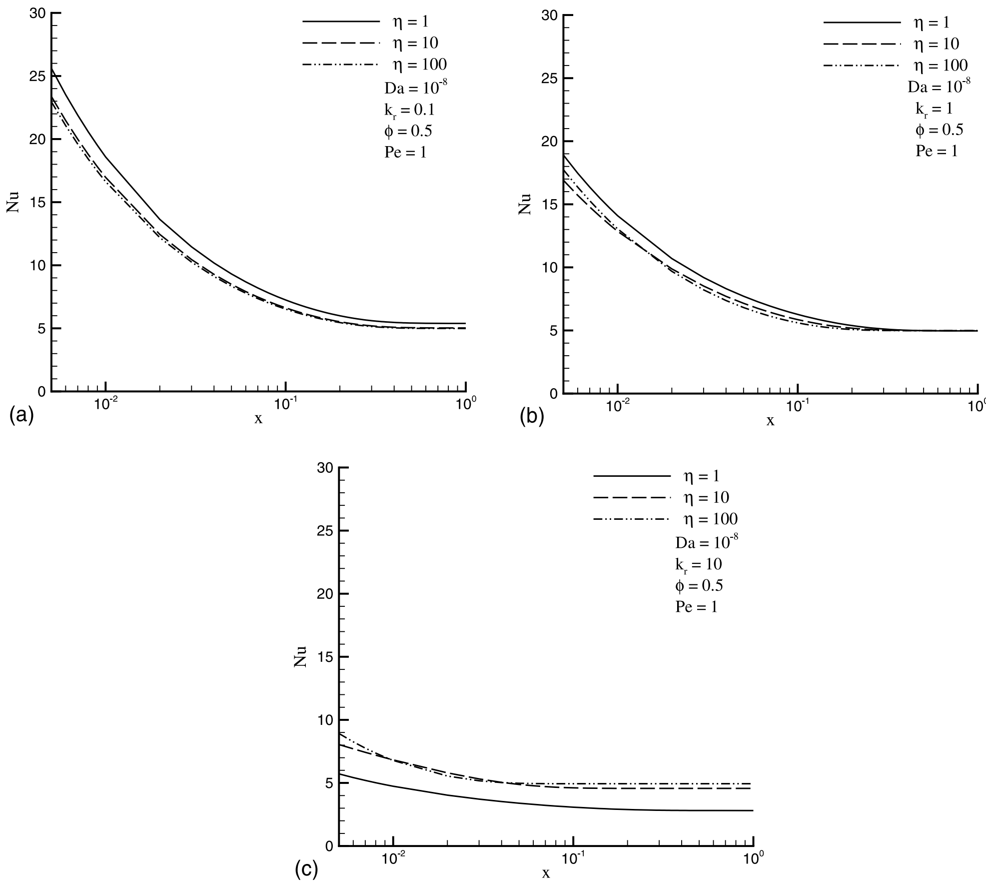

Fig. 2. Plots of local Nusselt number *Nu* versus longitudinal coordinate x for various values of the fluid–solid heat exchange parameter η, and conductivity ratios (a) $k_r = 0.1$, (b) $k_r = 1$, (c) $k_r = 10$. All results are for porosity $\phi = 0.5$, Péclet number $Pe = 1$, and Darcy number $Da = 10^{-8}$.

quently, we present results for a very limited range of parameters, chosen to illustrate the main trends. Also, we have been content to present just the local Nusselt number (from which the mean Nusselt number can be computed; see Eq. (41b)).

All our results are for a porous medium of porosity $\phi = 0.5$. In Figs. 2 and 3 we fix the value of Pe $(= 1)$, and we present, first for a relatively dense porous medium $(Da = 10^{-8})$ and then for a relatively sparse one $(Da = 10^{-3})$, plots of the local Nusselt number versus the longitudinal coordinate for representative values of the solid/fluid conductivity ratio k_r and the solid–fluid heat exchange parameter η. In the case of fully developed convection, the special cases $k_r = 1$ and very large η each correspond to local thermal equilibrium. We observe that for the developing convection situation there is a small LTNE effect apparent even when $k_r = 1$. The most prominent features shown in Figs. 2 and 3 are: (1) a variation in Darcy number has little effect on the Nusselt number, (2) the effect of the variation of heat exchange parameter is small, and the direction of change depends on the value of k_r: as η decreases from large values, the trend is for Nu to decrease if k_r is small and for Nu to increase if k_r is not small, and (3) the Nusselt number decreases markedly as the solid/fluid conductivity ratio increases.

In Fig. 4 we present the effect of variation of Péclet number. In the case of local thermal equilibrium, the dependence on Pe is confined to the scaling of the horizontal coordinate, but in the case of LTNE there is a further substantial effect. For a given value of $x = x^*/PeH$, the local Nusselt number increases as Pe increases, and this effect is particularly large if the solid/fluid conductivity ratio is small.

The constant-temperature thermal boundary conditions that we have imposed imply that there is local thermal equilibrium imposed at the boundary. It is to be expected that this restriction leads to a lower bound on the magnitude of the LTNE effects. In other words, with other boundary conditions (e.g. constant-flux

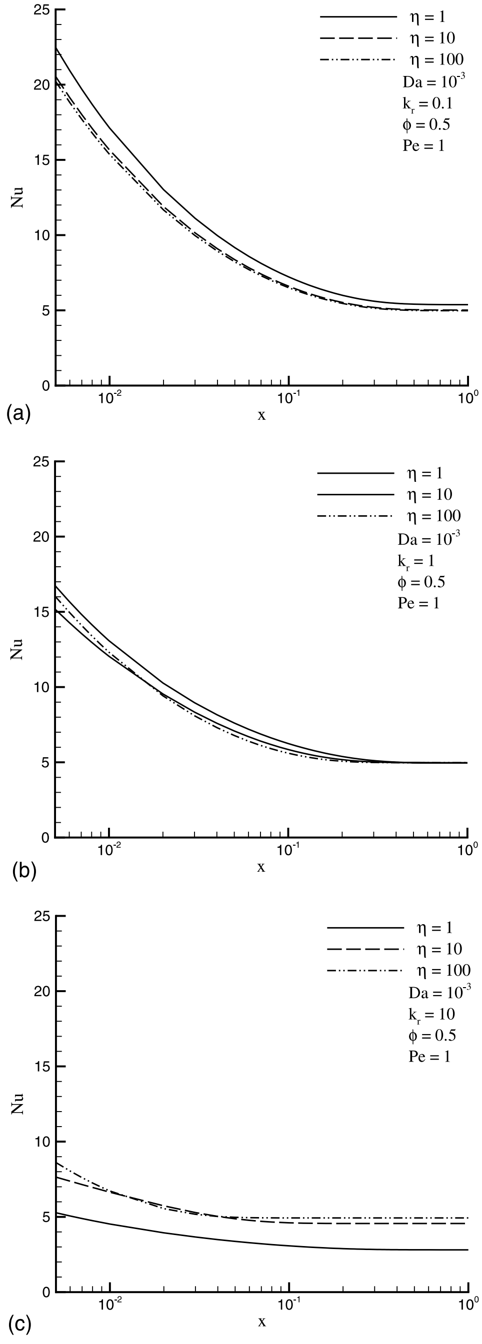

Fig. 3. As for Fig. 2, but for $Da = 10^{-3}$.

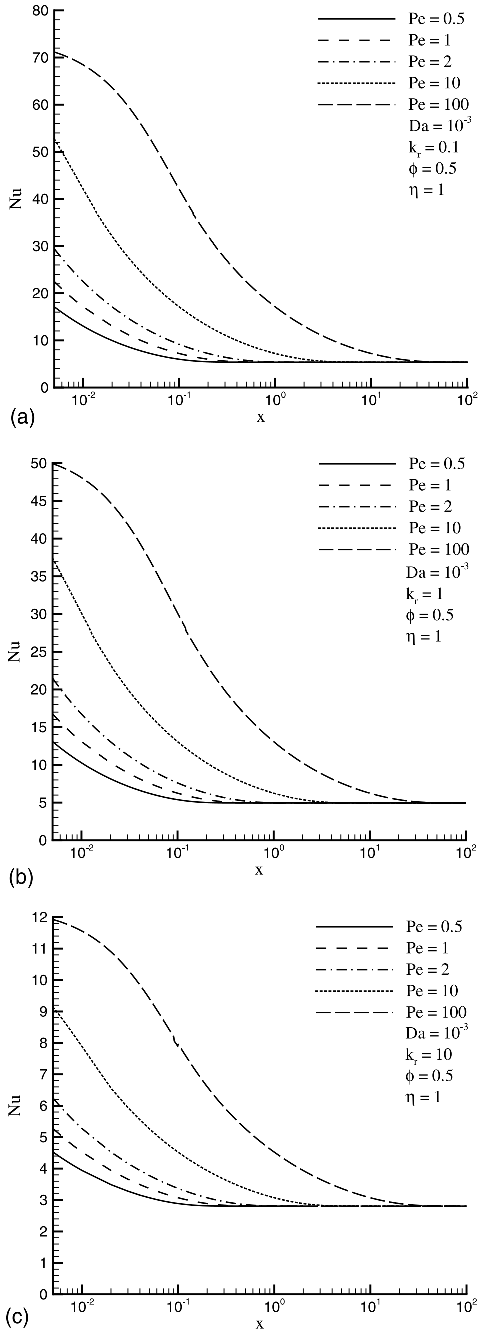

Fig. 4. Plots of local Nusselt number Nu versus longitudinal coordinate x for various values of the Péclet number Pe, and conductivity ratios (a) $k_r = 0.1$, (b) $k_r = 1$, (c) $k_r = 10$. All results are for porosity $\phi = 0.5$, fluid–solid heat exchange parameter $\eta = 1$, and Darcy number $Da = 10^{-3}$.

ones) LTNE is expected to have a more significant effect.

In this paper we have been concerned with the effect of LTNE on the heat transfer as represented by the Nusselt number. If one asks a different question, namely under what circumstances is the difference between fluid and solid temperatures significant, then an answer may be obtained from a comparison of terms in Eq. (22). The LNTE effect on temperature differences is insignificant if N_h is large compared with unity. From Eq. (19), one sees that if the conductivity ratio is of order unity then the LNTE effect on fluid–solid temperature differences is negligible if η/Pe is large compared with unity. This is in accord with the conclusions of Minkowycz et al. [8].

5. Conclusion

We have carried out a study on the effect of local thermal non-equilibrium on the thermal development of forced convection in a saturated porous medium confined in a channel between parallel plates on which the temperature is held constant. We have found that the local Nusselt number is strongly dependent on the values of the Péclet number and the solid/fluid conductivity ratio, and dependent to a lesser extent on the values of the solid–fluid exchange parameter and the Darcy number.

Acknowledgements

A.V.K. would like to acknowledge grant # 01/ER-12 awarded to him by the United Engineering Foundation and the support provided by the North Carolina Supercomputing Center (NCSC) under the Advanced Computing Resources Grant.

References

[1] D.A. Nield, A. Bejan, Convection in Porous Media, second ed., Springer-Verlag, New York, 1999, p. 192.
[2] G. Lauriat, R. Ghafir, Forced convection heat transfer in porous media, in: K. Vafai (Ed.), Handbook of Porous Media, Marcel Dekker, New York, 2000, pp. 201–267.
[3] D.A. Nield, A.V. Kuznetsov, M. Xiong, Thermally developing forced convection in a porous medium: parallel plate channel or circular tube with walls at constant temperature, J. Porous Media (submitted for publication).
[4] D.A. Nield, A.V. Kuznetsov, M. Xiong, Thermally developing forced convection in a porous medium: parallel plate channel or circular tube with walls at constant heat flux, J. Porous Media (to appear).
[5] D.A. Nield, Effects of local thermal nonequilibrium in steady convective processes in a saturated porous medium: Forced convection in a channel, J. Porous Media 1 (1998) 181–186.
[6] D.A. Nield, A.V. Kuznetsov, Local thermal nonequilibrium effects in forced convection in a porous medium channel: a conjugate problem, Int. J. Heat Mass Transfer 42 (1999) 3245–3252.
[7] A. Amiri, K. Vafai, Analysis of dispersion effects and non-thermal equilibrium non-Darcian variable, porosity incompressible flow through porous media, Int. J. Heat Mass Transfer 37 (1994) 939–954.
[8] W.J. Minkowycz, A. Haji-Sheik, K. Vafai, On departure from local thermal equilibrium in porous media due to a rapidly changing heat source: the Sparrow number, Int. J. Heat Mass Transfer 42 (1999) 3373–3385.